Preparation and Characterization of Organic Films by the Electrooxidation of a Thiophene Imine Derivative

F. R. Diaz,[1] M. A. del Valle,[1] F. Brovelli,[1] L. H. Tagle,[1] J. C. Bernede[2]

[1]*Laboratorio de Polímeros, Facultad de Química, Pontificia Universidad Católica de Chile, Vicuña Mackenna 4860, Santiago, Chile*
[2]*Groupe de Physique des Solides pour l'Electronique–Faculté des Sciences et des Techniques de Nantes, 2 Rue de la Houssinière, BP 92208, 44322, Nantes, Cedex 3, France*

Received 19 August 2002; accepted 16 November 2002

ABSTRACT: 2,2′-Dithienylimine was synthesized and electrochemically oxidized. The polymer was obtained on platinum or glass electrodes coated with tin oxide. The films were characterized with scanning electron microscopy, microprobes, and X-ray photoelectron spectroscopy. The coverage efficiency of the films was very high, but there were some morphological defects on the surfaces. Furthermore, there was some oxygen contamination not only on the surface but also in the bulk of the films. The nucleation and growth mechanisms responded to tridimensional instantaneous nucleation and bidimensional progressive nucleation contributions, which were consistent with the morphologies determined by scanning electron microscopy. The current–voltage characteristics exhibited a turn-on voltage of 5–6 V, which depended on the film thickness. © 2003 Wiley Periodicals, Inc. J Appl Polym Sci 89: 1614–1621, 2003

Key words: diodes; thin films

INTRODUCTION

Since the first report of electroluminescence (EL) from organic conjugate polymers,[1] effort has been devoted to the design of light-emitting devices. Organic light-emitting diodes (OLEDs) are composed of three or more layers:[2] the first is a transparent conductive oxide (TCO); the second is an organic active film, which can be a multilayer, for improved EL efficiency;[2–7] and the third is generally an aluminum film because of its relatively low work function and its good stability compared with that of metals with lower work functions, such as Ca.

Here we report an investigation on the electrical and electrochemical properties of an electrochemically oxidized thiophene imine derivative. For the active layer, we used a polymer based on this organic film (polymers with thiophene units have often been used in OLEDs[8]). We proceeded to central thiophene nucleus substitution, that is, to the incorporation of an organic function on the 2,2′-position. The organic function used was imine. The aim was to study the effect of such an organic function on the optoelectric properties of the polymer. The main characteristic of this substituted organic function was that it possessed π-electrons, which could induce a limited electronic delocalization on the new polymers. Such limited delocalization should decrease carrier leakage toward electrodes. Moreover, the effect of the chain modifications introduced here should be an increase in the band gap.

Correspondence to: F. R. Diaz (fdiaz@puc.cl).

Contract grant sponsor: Fondo de Desarrollo de Ciencia y Tecnología de Chile.

Contract grant sponsor: Programa Francés de Evaluation-Orientation de la Coopération Scientifique–Comisión Nacional de Investigación Científica y Tecnológica de Chile.

Journal of Applied Polymer Science, Vol. 89, 1614–1621 (2003)

EXPERIMENTAL

Monomer synthesis

2,2′-Dithienylimine (DTIM) was synthesized according to ref. 9, as shown in Scheme 1. Yellow-green crystals were obtained.

mp: 98–99°C. ^{1}H-NMR (200 MHz, $CDCl_3$, δ, ppm): 8.45 (1H, s), 7.50 (1H, dd), 7.46 (1H, dd), 7.10 (3H, m), 6.97 (1H, d). ^{13}C-NMR (50 MHz, $CDCl_3$, δ, ppm): 154.87, 142.31, 141.80, 132.12, 130.39, 127.94, 126.84, 123.37, 121.22. Elem. Anal. Found: C, 54.76%; H, 3.47%; N, 7.15%; S, 32.51%.

Electrochemical synthesis and characterization

The setup for cyclic voltammetry (CV) was previously described.[10] A polycrystalline, nonannealed Pt disc (geometrical area = 0.24 cm^2) and SnO_2-coated glass (TCO; geometrical area = 0.4 cm^2) were used as working electrodes; Ag/AgCl in a tetramethylammonium chloride solution was used as a reference electrode. Potentials with respect to the latter were corrected to

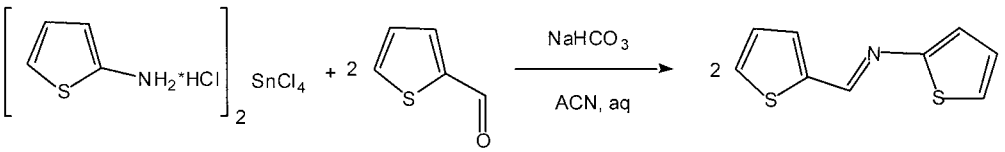

Scheme 1 Monomer synthesis.

that of a saturated calomel electrode (SCE).[11] A Pt gauze separated from the working electrode compartment by a glass frit was used as a counter electrode. Before each experiment, the working metal electrodes were polished with alumina slurry (particle size = 0.3 μm) on soft leather and afterward were washed with deionized water and anhydrous acetonitrile. Before all the experiments, the solutions were purged with high-purity argon, and an argon atmosphere was maintained over the solutions during the measurements. Anhydrous acetonitrile (Aldrich, St. Louis, MO) was stored in an atmosphere of dry argon and over 4-Å molecular sieves. Because thiophene and its derivatives should polymerize from highly anhydrous media[12] and so that minimum water contents would be ensured, the solvents were manipulated with syringes, and the supporting electrolyte, tetrabuthylammonium hexafluorophosphate (Bu_4NPF_6; Aldrich), was dried *in vacuo* at 60°C.

The nucleation and growth mechanism (NGM) study was carried out from solutions containing 0.025–0.1*M* monomer and 0.1*M* supporting electrolyte. In single potential step experiments, the electrode was first switched from 0.2 to 0.7 V for a period of 60 s. Polymerization was achieved by a further step to potentials between 1.50 and 1.60 V. The purpose of this potential–time program was reported elsewhere.[13] In the CV experiments, the potential was successively scanned between −0.9 and 2.6 V at 100 mV s^{-1}. Chronoamperometric and CV experiments were acquired with a BAS (West Lafayette, IN) CV-50W.

The TCO used was commercial SnO_2 (Solems, Palaiseau, France). The whole glass substrate was covered, and so some SnO_2 needed to be removed. After a broad line of 2 mm was masked, SnO_2 was etched with Zn and HCl.[14] Then, the substrates were cleaned with an H_2O_2 treatment according to a process described by Osada et al.,[15] which corresponded to the first solution (SC1) of the RCA (Princeton, NJ) process first described by Kern and Puotinen.[16] The substrates were treated with an H_2O–H_2O_2 (30%)/NH_4OH (25%) solution (5:1:1 v/v/v) at 80°C for 20 min, and this was followed by rinsing with boiling distilled water for 5 min. The use of boiling water has been proved to be helpful for obtaining impurity-free surfaces.[17]

Surface characterization

The observations of the surface morphology and the cross sections of the layers were performed with a JEOL (Peabody, MA) 6400F field-effect scanning electron microscope. Electron probe microanalysis was used for qualitative analysis.

Electron spectroscopy for chemical analysis (ESCA) measurements were performed with a Leybold spectrometer at the University of Nantes Centre National de la Recherche Scientifique. ESCA was used for X-ray photoelectron spectroscopy (XPS) measurements. The X-ray source was a magnesium cathode (1253.6 eV) operating at 10 kV and 10 mA. The energy resolution was 1 eV at a pass energy of 50 eV. High-resolution scans with a good signal-to-noise ratio were obtained in the C1s, S2p, and N1s regions of the spectrum. The quantitative studies were based on the determination of the C1s, S2p, and N1s peaks areas with 0.2, 0.44, and 0.6, respectively, as sensitive factors; the sensitivity factors were given by the manufacturer. The decomposition of the XPS peaks into different components and the quantitative interpretation were made after the subtraction of the background with the Shirley method.[18] The developed curve-fitting programs permitted the variation of parameters such as the Gaussian–Lorentzian ratio, the full width at half-maximum (fwhm), and the position and intensity of the contributions. These parameters were optimized by the curve-fitting program for the best fit.

Electrical characterization

OLEDs were prepared by the deposition of aluminum *in vacuo* on top of a polymeric film deposited onto a glass substrate coated with SnO_2. The current–voltage (I–V) curves were measured with a Keithley (Cleveland, OH) 617 programmable electrometer, a Keithley 2000 multimeter, and a Lambda (Rochester, NY) IEEE-488 programmable power supply (model LLS6060-GPIB) interfaced to an IBM personal computer. EL was detected through the transparent SnO_2 electrode and glass. The light output was detected with a silicon photodiode and a Keithley 617 electrometer.

RESULTS AND DISCUSSION

Electrochemical monomer characterization

The anodic voltammetric profile of this monomer is shown in Figure 1. From this profile, it is possible to distinguish three oxidation peaks between 1.6 and 2.3 V, the two main ones corresponding to the oxidation of the rings and the third to the functional group. As

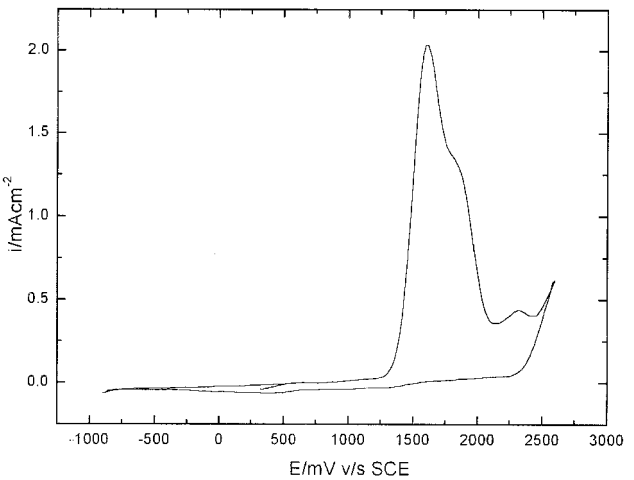

Figure 1 CV profiles of DTIM (interface = Pt/0.025*M* DTIM + 0.1*M* $TBAPF_6$ in CH_3CN; scan rate = 100 mV s^{-1}).

we previously reported, the electron densities determined by *ab initio* Hartree–Fock calculations are very similar for the sulfur atoms in both rings, but there are small differences due to the electron-withdrawing effect and/or electron-donating effect through the group acting as a bridge, besides the conjugation effect produced between both rings.[9] Therefore, the effect of the group acting as a bridge between the thiophene rings is shown by a significant variation of the peak potentials with respect to thiophene.

An analysis of the electron densities indicates that, although there is a conjugation between the rings, the main electron density is concentrated on the sulfur atom next to the nitrogen, which possesses an electron pair that can resonate with the ring. The electron density distribution determined in other thienyl derivatives shows that, in this case, there has been an inversion in the electron densities in the carbon atoms acting as bridges with the imine group. One could, therefore, expect that the ring substituted by nitrogen at the 8-position should be more reactive. Nevertheless, the oxidation of the imine group cannot be ignored. In symmetric molecules, it is expected that the decrease in the oxidation potential will be more pronounced. However, the energy minimization shows that, in some cases, the deviation of the planes in the rings causes a decrease in the π-electrons overlapping, and this would explain the loss of electrochemical reversibility shown by these molecules in solution. According to the electron densities and the voltammograms, the oxidation of this molecule would involve heterocyclic rings, although the competitive or consecutive oxidation of the functional group could also be taking place.[9]

As can be seen in Figure 2, the growth profile of the deposit is strongly influenced by the anodic inversion potential: when it is 2.2 V, a decrease in the oxidation current is observed, as well as an anodic shift of the peak. However, when the anodic limit is extended, a more pronounced decrease in the current is observed. This implies that the polymerization potential modifies the conducting properties of the deposit. Under these circumstances, the deposit generated at a more anodic potential would be less conducting because the polymeric structure would be branched, losing the conjugation between the thiophene rings, on account of the possibility of oxidation of not only the thio-

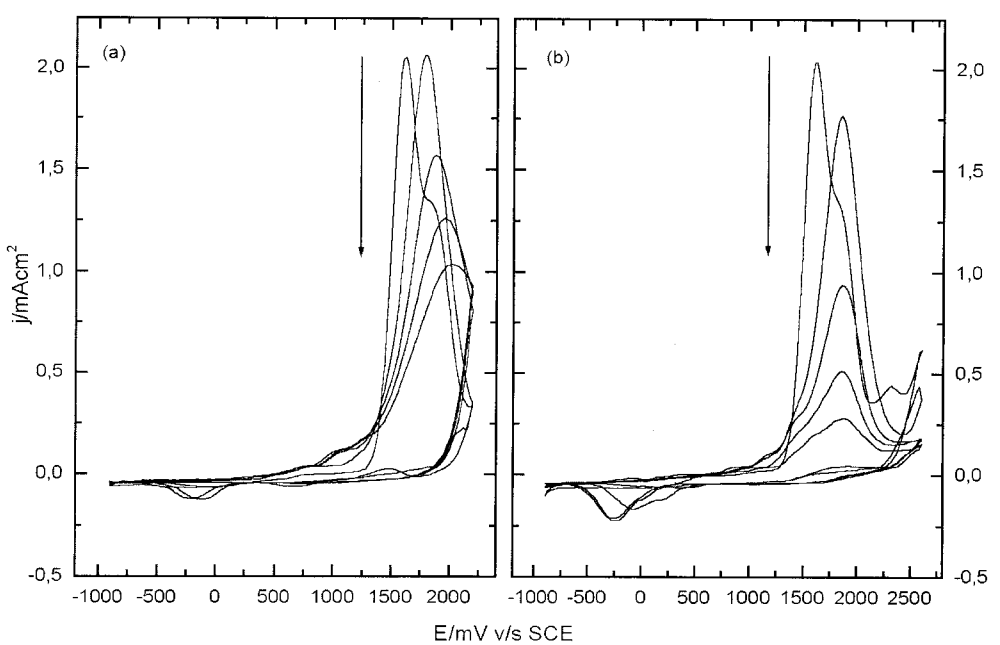

Figure 2 CV profiles during the electrooxidation of DTIM (interface = Pt/0.05*M* DTIM + 0.1*M* Bu_4PF_6 in CH_3CN; scan rate = 100 mV s^{-1}) showing the effect of the inversion potential (E): (a) 2.2 and (b) 2.6 V.

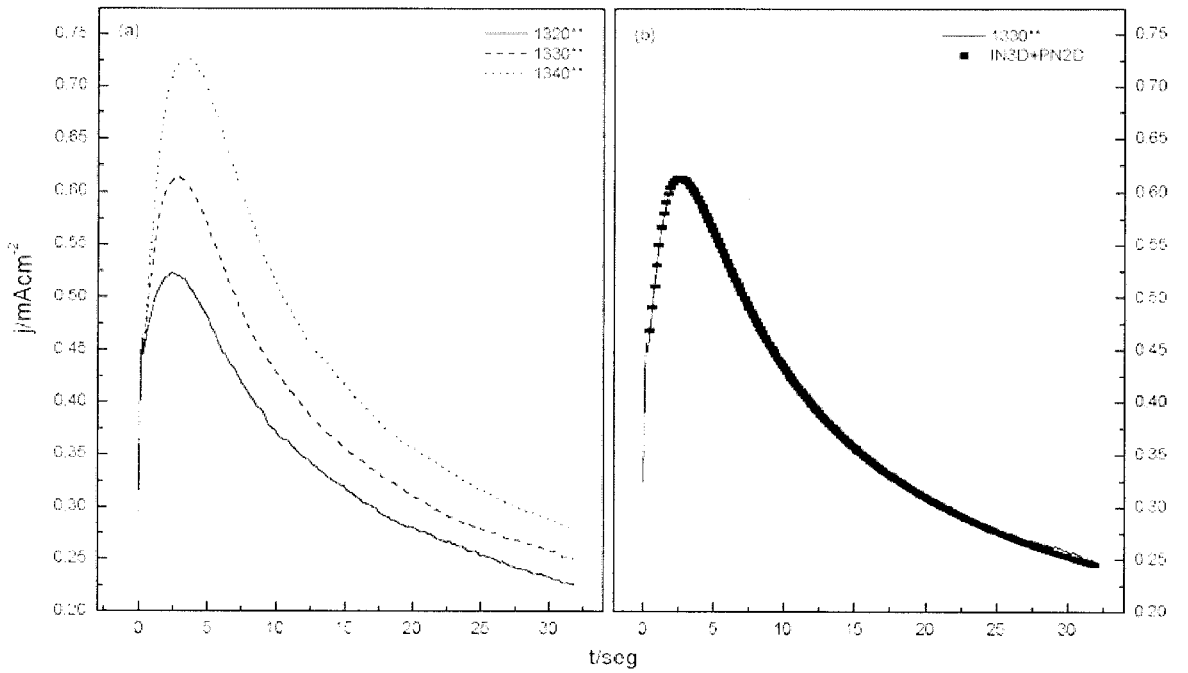

Figure 3 Current–time transients for DTIM electrooxidation at different potentials (interface = Pt/0.025*M* DTIM + 0.1*M* Bu_4PF_6 in CH_3CN): (a) experimental transients and (b) experimental transients fitted by means of eq. (1). The IN3D and PN2D contributions were calculated from the respective terms of the same equation.

phene rings but also the functional groups (overoxidation).

NGM

With the aim of establishing the NGM, potentiostatic pulse experiments were carried out with electrolytic solutions containing the monomer. The potentiostatic pulses were recorded at potentials at which the current increase occurred during the voltammetric cycle (Fig. 3). The current/time (i/t) transients were deconvoluted according to various mechanisms proposed in the literature.[19,20] For each case, the analysis of the current density variation considered different models, which operated simultaneously or successively. In all the experiments performed, only the effect of the monomer concentration was taken into account; the type and concentration of the support electrolyte were kept constant.

In the literature, several NGMs have been proposed for the electropolymerization of thiophene and its derivatives,[13,21,22] and it has been found that more than one contribution can operate simultaneously or successively.[10,12] In this case, the model best fitting the transients is composed of a tridimensional instantaneous nucleation (IN3D) contribution, controlled by charge transfer, and a bidimensional progressive nucleation (PN2D) contribution, controlled by diffusion. The equation that describes the complete transient for the analyzed potentials is

$$j = a[1 - \exp(-bt^2)] + ct^{-0.5}[1 - \exp(-dt)] \quad (1)$$

The constants a, b, c, and d can be described as follows:

$$a = (nFk_3') \quad (2)$$

$$b = (\pi N_{3D} M^2 k_3^2)/\rho^2 \quad (3)$$

$$c = (nFD^{0.5}C_\infty)/(\pi^{0.5}) \quad (4)$$

$$d = N_0 \pi K D \quad (5)$$

where

$$K = (8\pi C_\infty M \rho^{-0.5})^{0.5} \quad (6)$$

n, F, M, and ρ represent the electron number, Faraday constant, molecular weight, and density, respectively; N_{3D} corresponds to the number of three-dimensional (3D) nuclei formed at $t = 0$; k_3 and k_3' correspond to the rate constants of the 3D nuclei for growth parallel and perpendicular to the surface, respectively; and D and C_∞ are the diffusion coefficient and monomer concentration, respectively, and N_0 are the nuclei formed at $t = 0$.

The parameters evaluated from the variables involved in each contribution are summarized in Table I. The IN3D contribution would involve only short-chain oligomers, as proposed for the electropolymerization of thiophene and 3-methylthiophene.[12,22] This

TABLE I
Effect of the Experimental Parameters on the Constants Evaluated from Eq. (1)

DTIM (M)	E (mV)	a (mA cm^{-2})	b (s^{-2})	c (mA cm^{-2} s$^{-1/2}$)	d (s^{-1})
0.025	1320	0.02748	0.00763	1.14776	0.55068
	1330	0.05977	0.16011	1.14776	0.63997
	1340	0.12417	0.26247	1.14776	0.71540
0.05	1320	0.13187	0.11914	1.10640	2.30780
	1330	0.13187	0.12284	1.10640	2.31540
	1340	0.13187	0.12284	1.10640	2.53180
0.1	1320	0.04233	0.05531	0.43023	0.89937
	1330	0.06294	0.19251	0.43023	1.1715
	1340	0.14000	1.24470	0.43023	1.1903

E = potential.

effect has been explained by the strong interaction existing between the monomer or oligomers with the metallic surface, which favors the formation of two-dimensional (2D) layers.[23] It can also be seen that for $t > 4$ s, the IN3D contribution decreases because the 3D nuclei start to coalesce, and the only important growth process is the 2D one controlled by diffusion. This contribution dominates practically the whole region for times longer than 5 s, within which the net current decreases gradually. This type of behavior can be attributed to layer-by-layer 2D growth, with uniform layers of constant thickness.

Nevertheless, the change in the electrode substrate involves changes in the NGM of polythiophene.[24] In the first stage of oxidation, the oxidation of the substrate takes place at a potential at which the formation of a polymer monolayer occurs. The formation of a bulk deposit occurs by instantaneous nucleation and tridimensional growth of the polymer on the monolayer. Other studies have suggested that the polymerization process follows a current/(time)^2 (I–t^2) relation, which is consistent with instantaneous nucleation and tridimensional growth.[21] By a comparison with other results,[25] it can also be found that the electropolymerization at low potentials is controlled by charge transfer, whereas at high potentials, the process is controlled by diffusion. Moreover, after a certain time lapse, the main contribution is controlled by diffusion, and this is consistent with the formation of a region with a high oligomeric density, such as has been proposed from the electropolymerization mechanism of polythiophene.[12] In any case, the difference in the NGMs of various thienyl derivatives can be explained in terms of electronic and steric effects of the functional groups acting as bridges.

Surface analysis

The visualization of the surface morphology has shown that there is a high coverage efficiency of the deposition process [Fig. 4(a)]. No pinholes are visible after only five voltammetric cycles, but some topological heterogeneities are visible on the surfaces of the films. At a higher magnification [Fig. 4(b)], it can be seen that the films exhibit the cauliflower-like aspect traditionally found for polythiophene.[26]

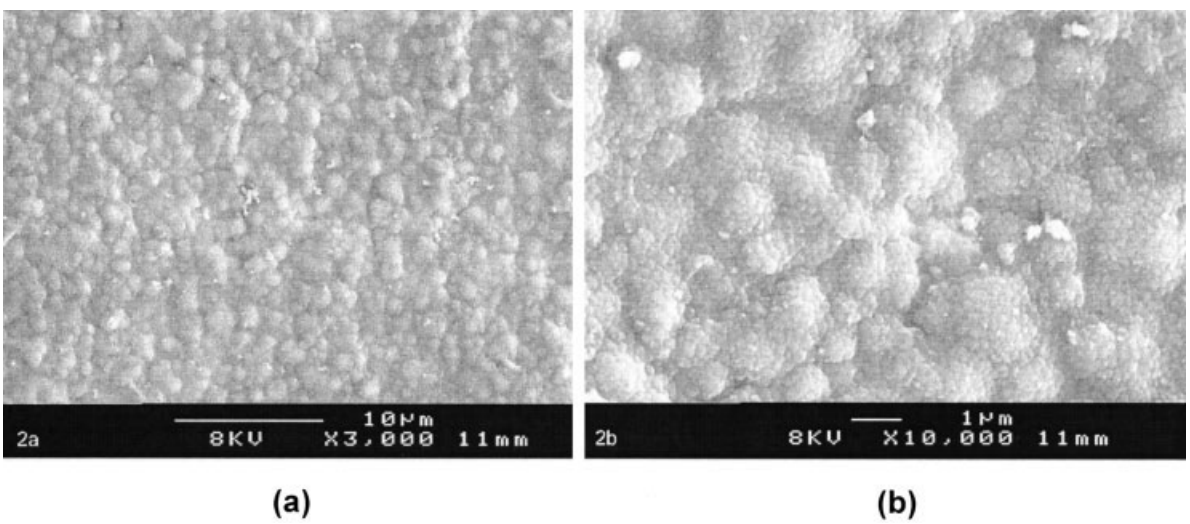

Figure 4 Microphotographs of polyDTIM deposited by potentiodynamic scans on Pt electrodes: (a) 3000× and (b) 10,000×.

TABLE II
XPS Data from the Decomposed Spectrum of polyDTIM Obtained from Pt/0.05*M* DTIM + 0.1*M* Bu_4PF_6 in CH_3CN by 25 Voltammetric Cycles at a Scan Rate of 100 mV s^{-1}

			C1s			N1s			O1s		S2p	X
Theory (%)			75			8.5					16.5	
Species	C—C	C—S, N, OH		C═O	COOH	N		N^+ C—OH		C═O	S	F
Experimental (%)			60			6			27.5		5.5	1
Potential Difference (eV)	285.1	286.6		288.2	289.6	399		401 530.3		532.1	164.8	
Area (%)	63.9	22.4		8.9	4.8	74.1		25.9 36.1		41.1	100	
fwhm			1.8			2.3			2		1.4	

The surface composition has been estimated by XPS. In this case, there is some oxygen contamination (Table II). These extra atoms can be related to air, electrolyte salt, and/or solvent contamination. In some samples, some dopant (fluorine) is present. However, the atomic dopant relative concentrations are often small. The undoping possibility is very important for OLED applications because it has been shown that the photoluminescence effect usually falls down in the presence of dopant counterions.

In the decomposition of XPS peaks (Fig. 5), it should be noted that in this polymer there is some superficial oxygen contamination. The decomposition of the C1s peak [Fig. 5(a)] shows that four contributions are necessary to obtain a good fit between experimental and theoretical curves. The first contribution, situated at 285.1 eV, can be attributed to the C—C bond. This C—C binding energy has been taken as a reference, as is often the case.[27] The second one at 286.6 eV is more difficult to attribute. Its binding energy is a little too high to be attributed to C—S but is a little too low to be attributed to C—OH contamination. In fact, it corresponds to C—N. However, the relative atomic value of the contribution (22 atom %) cannot be attributed to C—N only; therefore, it should be attributed to a mixture of C—S, C—N, and C—OH. The third contribution, situated at 288.2 eV, corresponds to the C═O bonds, but there may also be a surface contamination contribution. The fourth peak can be assigned to COOH surface contamination. The O1s peak can be decomposed into two contributions. The first one, situated at about 530.3 eV, corresponds to the degraded C═O bonds of the polymer, and the second one, at 532.1 eV, can be assigned to contamination. It may correspond to some C—OH contamination and also to some adsorbed H_2O.[28]

The S2p line corresponds to a doublet. The main contribution, situated at 164.8 eV, corresponds to C—S bonds of the polymer. The decomposition of the N1s peak [Fig. 5(c)] shows that two contributions are necessary to obtain a good curve fit. The first contribution, located at 399 eV, corresponds to covalent nitro-

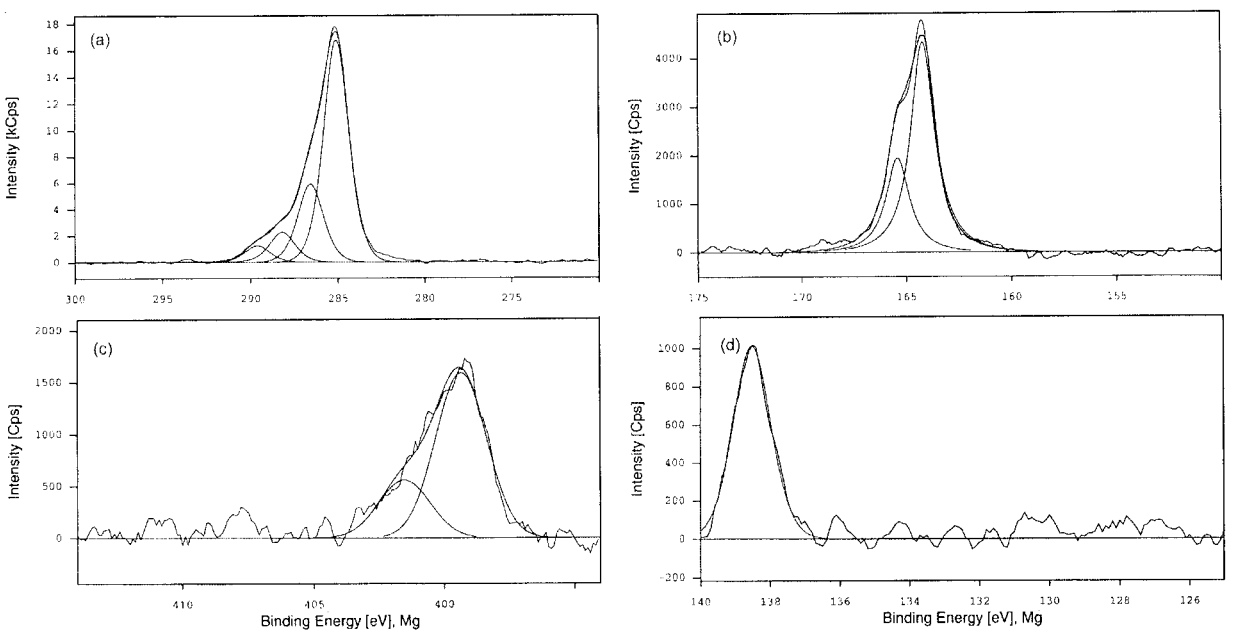

Figure 5 Decomposed XPS spectra of polyDTIM showing the different contributions of the elements in the polymer: (a) C1s, (b) S2p, (c) N1s, and (d) P2p.

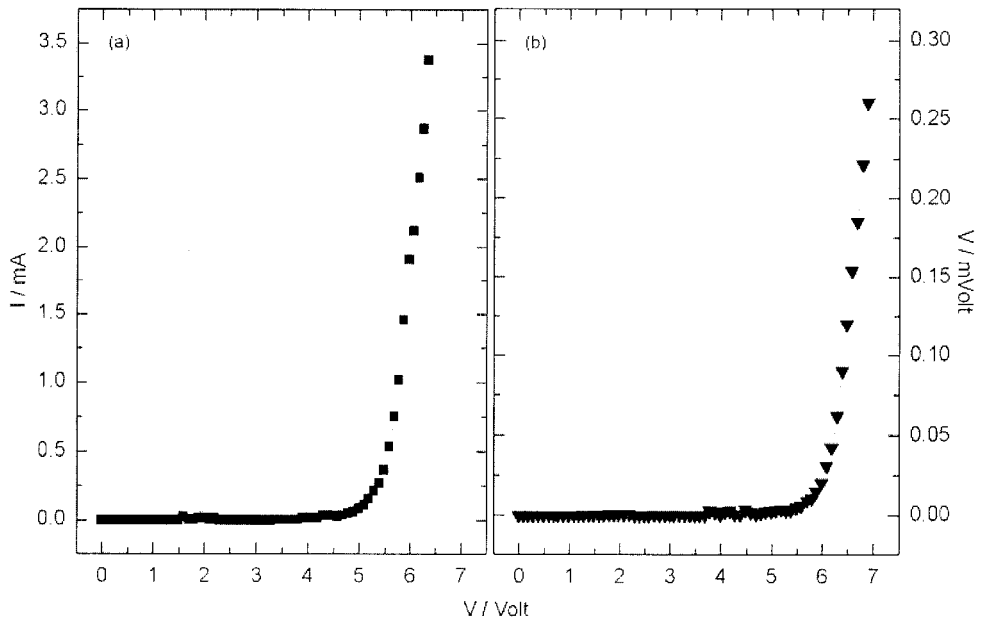

Figure 6 I–V characteristic curves of TCO/polyDTIM/aluminum devices at room temperature.

gen. The second contribution, at 401 eV, can be attributed to positively charged nitrogen from the supporting electrolyte.

After 1 min of etching, for sulfur, only the contribution corresponding to C—S bonds is still present, and this shows that S oxidation is only a surface phenomenon.

I–V curves

The electrical behavior of devices measured under ambient conditions under a forward bias follows a characteristic diode behavior [Fig. 6(a)]; the turn-on voltage is a little larger than that of other devices prepared with dithienyl derivatives.[29] The effect of the group acting as a bridge between the rings on the turn-on voltage is directly related to its electron-donating effect, causing a shift in the turn-on voltage toward higher values. When the applied bias to a new diode is slowly increased, the behavior is first ohmic for a low voltage, but the current varies widely between devices. When the potential increases, the current often becomes noisy in the range of 1–4 V. Often the current becomes superlinear and then switches off. In that domain, the current may vary by several orders of magnitude between devices, and more than one switching can be evidenced. When the turn-on voltage is achieved, the noise disappears, and the current increases exponentially with the voltage [Fig. 6(a)].

Figure 6(b) shows the EL characteristics obtained for a device with an indium tin oxide/polymer/aluminum configuration. The light intensity, measured as the photodiode tension, increases rapidly with a bias greater than 6 V, and this is typical of rectifying characteristics. Both curves show the same shape. EL appears after a current increase in the forward direction. This indicates that the EL and I–V mechanisms are the same.

The understanding of the electrical process appears to be very important for achieving highly performing diodes. For the I–V characteristics, the dominant conduction mechanism cannot be ohmic, trap-free and space-charge-limited, or purely tunneling injection. The temperature and thickness dependence observed in our previous studies indicate that it must be either thermionic emission or thermally assisted tunneling.[30,31]

In the low potential range, the high current flow and switching effects cannot be satisfactorily explained by the usual models for charge carrier injection and/or transport. Moreover, some heterogeneity is present on the surfaces of the polymeric films. Also, although the samples are cooled with liquid nitrogen during aluminum deposition, some metal diffusion could take place. As a result, some leakage paths could be induced. These paths can justify the large current variation from one sample to another for small potentials; in that case, the switching effect can be related to the burnout of these leakage paths.

CONCLUSIONS

A polymer based on a thiophene imine derivative (polyDTIM) was electrochemically synthesized, and it showed a very high electrode coverage efficiency; however, some topological heterogeneities were visible on the surface. The morphology was consistent with the established NGM.

The undoping possibility of these films was corroborated by XPS, and it is very important for applications in OLEDs. Therefore, TCO/polyDTIM/aluminum structures based on this new polymer were assayed. The I–V characteristics exhibited a turn-on voltage of 5–6 V that depended on the film thickness, and the EL response appeared above 6 V.

For increased luminescence of the device based on DTIM, a second organic film, an electron-transport layer, was deposited on the polyDTIM layer before aluminum deposition.

References

1. Burroughes, J. H.; Bradly, D. D. C.; Brown, A. R.; Marks, R. N.; Mackay, K.; Friend, R. H.; Burmond, P. L.; Holmes, A. B. Nature 1990, 374, 539.
2. Halls, J. J. M.; Baigent, D. R.; Cacialli, F.; Greenham, N. C.; Friend, R. H.; Moratti, S. C.; Holmes, A. B. Thin Solid Films 1996, 276, 13.
3. Hosokana, C.; Higashi, H.; Nahamura, H.; Kusumoto, T. Appl Phys Lett 1995, 67, 3853.
4. Vestweber, H.; Rie, W. Synth Met 1997, 91, 181.
5. Zhang, Z.-L.; Jiang, X.-Y.; Xu, S.-H.; Nagatomo, J.; Omoto, O. Synth Met 1997, 91, 131.
6. Jolinat, P.; Clergereaux, R.; Farenc, J.; Destruel, P. J Appl Phys 1998, 31, 1.
7. Clergeaux, R.; Jolinat, P.; Nguyen, T. P.; Destruel, P.; Farenc, J. J Chim Phys 1998, 95, 1347.
8. Nguyen, T. P.; Molinié, P.; Destruel, P. In Handbook of Advanced Electronic and Photonic Materials and Devices; Nalwa, H. S., Ed.; Academic: San Diego, 2000.
9. Brovelli, F.; del Valle, M. A.; Díaz, F. R.; Bernède, J. C. Bol Soc Chil Qui 2001, 46, 319.
10. Córdova, R.; del Valle, M. A.; Gómez, H.; Schrebler, R. J Electroanal Chem 1994, 377, 75.
11. East, G. A.; del Valle, M. A. J Chem Educ 200, 77, 97.
12. Schrebler, R.; Grez, P.; Cury, P.; Veas, C.; Merino, M.; Gómez, H.; Córdova, R.; del Valle, M. A. J Electroanal Chem 1997, 430, 77.
13. Li, F.; Albery, W. J. Electrochim Acta 1992, 37, 393.
14. Gordon, G. Mater Res Soc Symp Proc 1996, 426, 419.
15. Osada, T.; Kugler, T.; Bröms, P.; Salaneck, W. S. Synth Met 1998, 96, 77.
16. Kern, W.; Puotinen, D. A. RCA Rev 1970, 187.
17. Messoussi, R. Ph.D. Thesis, Université de Kénitra, Kénitra, Morocco, 1998.
18. Shirley, A. Phys Rev B 1972, 5, 4709.
19. A Guide to the Study of Electrode Kinetics; Academic: London, 1972.
20. Southampton Electrochemistry Group. Instrumental Methods in Electrochemistry; Ellis Horwood: Chichester, England, 1985.
21. Downward, A. R.; Pletcher, D. J Electroanal Chem 1987, 220, 351.
22. Hillman, A. R.; Mallen, E. J Electroanal Chem 1988, 243, 403.
23. Obretenov, W.; Schmidt, H.; Lorenz, W. J.; Staikov, G.; Budevski, E.; Carnal, D.; Miller, U.; Siegenthaler, H.; Schmidt, E. J Electrochem Soc 1993, 140, 692.
24. Gui, J. Y.; Stern, D. A.; Lu, F.; Hubbard, A. T. J Electroanal Chem 1991, 305, 37.
25. Zhang, W.; Plietch, W.; Koßmehl, G. Electrochim Acta 1997, 42, 1653.
26. Samir, F. Ph.D. Thesis, University of Nantes, 1994.
27. Beamson, G.; Briggs, D. The Scienta ESCA 300 Database; Wiley: Chichester, England, 1992.
28. Kil, J. S.; Ho, P. K. H.; Thomas, D. S.; Friend, R. H.; Cocialli, F.; Bao, G. W.; Li, S. F. Y. Chem Phys Lett 1999, 315, 307.
29. Brovelli, F.; Díaz, F. R.; del Valle, M. A.; Bernède, J. C.; Molinie, P. Synth Met 2001, 122, 123.
30. Brovelli, F.; Bernède, J. C.; Marsillac, S.; Díaz, F. R.; del Valle, M. A.; Beaudouin, C. J Mater Sci, to appear.
31. Camplele, J.; Bradley, D. D. C.; Lawbender, J.; Sokolowski, M. J Appl Phys 1999, 86, 5004.